Exposure-Gate Beam-Mask Demonstration: Support-Weighted Transmission and Surtea Boundary Valuation

Peter M. Austin
Information Physics Institute

Revised 24 May 2026

Numerical companion note for the RSG exposure-gate protocol.

Abstract

This short note records two reproducible demonstrations of the exposure-gate idea used in Recursive Survival Geometry. The first demonstration is a synthetic optical beam-mask example. An incident beam image is fixed before the reveal, several lossy masks are fixed, and the exposure weight W is computed by summing the incident support inside each mask. The exposure-gated transmission $G = \exp(-\eta W)$ is then compared with a path-only attenuation control $G_{\mathrm{path}} = \exp(-\eta)$. The second demonstration repeats the same idea using Surtea-style finite support data. A valued D-cell universe is assigned a valuation ν_D; each support has an interior, closure, and boundary; and boundary valuation defines the exposure weight $W_X = \nu_D(\mathrm{bd}_D X)/\nu_D(\mathrm{cl}_D X)$. Neither demonstration is presented as an empirical proof of RSG. The purpose is narrower: to show how W can be fixed before output comparison, how the gate multiplies prepared representation before normalisation, and how a support-based exposure law differs from ordinary path-only attenuation.

Keywords: Recursive Survival Geometry; Exposure Gate; Support Valuation; Beam Mask; Surtea Support; Analogue Readout.

1 Claim Status

The demonstrations in this note are deliberately modest. They do not derive a new optical law, a new probability law, or a new matter law. They show how an exposure factor can be computed from already declared support data and then used as a transmission multiplier.

Claim	Status	Failure condition
W can be fixed from an incident beam image and mask geometry.	Operational definition in the beam-mask model.	Fails if masks, image support, or normalisation are changed after the reveal.
$G = \exp(-\eta W)$ is an exposure-gate transmission.	Model rule, declared before comparison.	Fails as an RSG-specific test if it does not improve on the path-only control in the declared positive-control regime.

Claim	Status	Failure condition
$W_X = \nu_D(\mathrm{bd}_D X)/\nu_D(\mathrm{cl}_D X)$ is a Surtea boundary exposure.	Support-valuation definition.	Fails if ν_D, bd_D, or cl_D are altered after inspection.
The rendered figures support a future manuscript insert.	Reproducibility and illustration claim.	Fails if the scripts cannot regenerate the displayed metrics and figures.

2 Beam-Mask Exposure

The beam-mask example begins with a fixed incident image $I_{\mathrm{in}}(x, y)$ and a family of fixed lossy masks M_m. The exposure weight of mask m is defined by the support fraction

$$W_m = \frac{\sum_{(x,y)\in M_m} I_{\mathrm{in}}(x, y)}{\sum_{(x,y)} I_{\mathrm{in}}(x, y)}. \tag{1}$$

This is the important protocol point. W_m is not fitted to the measured output. It is computed from the incident support before the held-out transmission values are compared.

The path-only attenuation control treats every mask as equally exposed:

$$T_{\mathrm{path}} = \exp(-\eta). \tag{2}$$

The exposure-gated model instead uses

$$T_m^{\mathrm{gate}} = \exp(-\eta W_m). \tag{3}$$

For the rendered example, $\eta = 1.05$. The held-out values are synthetic readouts generated with small locked noise around the exposure-gated law. A laboratory replacement would keep the same calculation of W_m, replace $\widehat{T}_m$ with measured detector readings, and compare both models under a preregistered error rule.

Table 2: Beam-mask metrics generated by the accompanying Python script.

Mask	W	$\widehat{T}$	T_{path}	T_{gate}	e_{path}	e_{gate}
far left	0.086	0.917	0.350	0.914	0.567	0.004
left shoulder	0.234	0.791	0.350	0.782	0.441	0.009
centre	0.300	0.735	0.350	0.730	0.385	0.006
right shoulder	0.198	0.804	0.350	0.812	0.455	0.008
far right	0.065	0.930	0.350	0.934	0.580	0.004

The comparison is intentionally simple. The total absolute error is 2.428 for the path-only control and 0.030 for the exposure-gated prediction. The RMSE is 0.491 for the path-only control and 0.006 for the exposure-gated prediction. This does not prove RSG. It shows, inside a locked positive-control construction, why a support-weighted exposure law is not the same object as ordinary path-only attenuation.

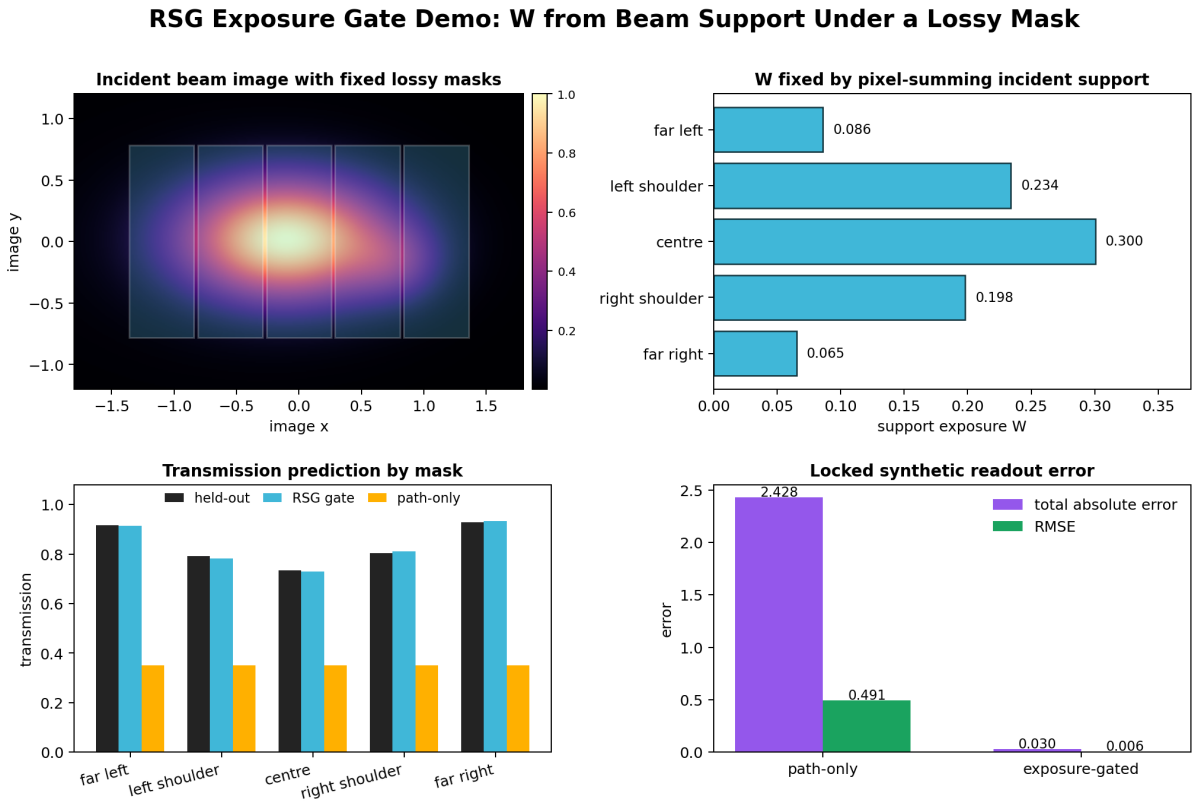

Figure 1: Beam-mask exposure demonstration. The incident support and masks determine W before the held-out transmission comparison. The exposure-gated model uses $T_m = \exp(-\eta W_m)$, while the path-only control uses the same attenuation for every mask.

3 Surtea Support Version

The Surtea-style version replaces the beam image with a valued finite support universe. Let

$$U = (M, D) \tag{4}$$

be a finite D-cell universe, and let ν_D be a positive valuation on D-cells. For a support $X \subseteq M$, define an interior, closure, and boundary by

$$\mathrm{bd}_D(X) = \mathrm{cl}_D(X) \setminus \mathrm{int}_D(X). \tag{5}$$

The boundary exposure used in the demonstration is

$$W_X = \frac{\nu_D(\mathrm{bd}_D X)}{\nu_D(\mathrm{cl}_D X)}. \tag{6}$$

The corresponding gate is

$$G_X = \exp(-\eta W_X). \tag{7}$$

This turns the Surtea support distinction into an operational exposure law. Compact supports have more proper interior share and lower boundary exposure. Hollow or fragmented supports expose more of their valued closure to the boundary channel. The model does not claim that boundary exposure is mass, gravity, or matter. It says only that boundary valuation can be used as a declared exposure variable before a survival gate is applied.

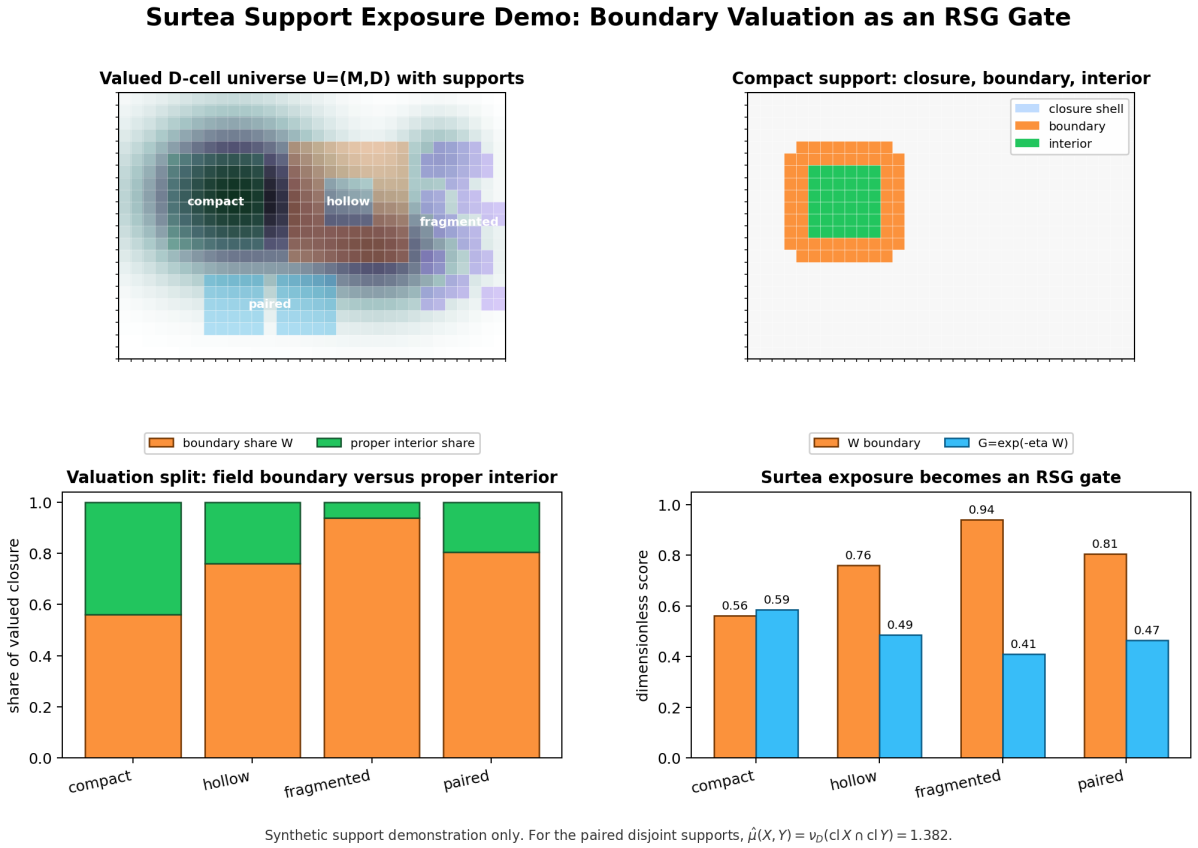

Figure 2: Surtea support exposure demonstration. A valued D-cell universe is decomposed into closure, boundary, and interior. Boundary valuation supplies W_X, and $G_X = \exp(-\eta W_X)$ supplies the survival-gate transmission.

Here $\nu_{\mathrm{cl}} = \nu_D(\mathrm{cl}_D X)$, $\nu_{\mathrm{int}} = \nu_D(\mathrm{int}_D X)$, and $\nu_{\mathrm{bd}} = \nu_D(\mathrm{bd}_D X)$.

Table 3: Surtea support-gate metrics generated by the accompanying Python script.

Support	ν_{cl}	ν_{int}	ν_{bd}	W_X	G_X	$\hat{\mu}$
compact	70.603	30.923	39.680	0.562	0.586	0.000
hollow	71.860	17.276	54.584	0.760	0.486	0.000
fragmented	34.926	2.110	32.816	0.940	0.410	0.000
paired	25.556	4.961	20.595	0.806	0.465	1.382

For the paired disjoint supports, the script also computes the interaction measure

$$\hat{\mu}(X,Y) = \nu_D(\mathrm{cl}_D\, X \cap \mathrm{cl}_D\, Y), \qquad X \cap Y = \varnothing. \tag{8}$$

In the rendered case, $\hat{\mu}(X,Y) = 1.382$. This gives a concrete place for the Surtea interaction measure: it is not the same as the survival gate, but it can be carried alongside the boundary exposure when the support geometry is part of the declared model.

4 Catalogue of Numerical Demonstrations

The probability note and the v1.4 revision contain several small numerical demonstrations of the same gate logic [3, **?**]. The earlier rejected v1.2 manuscript is cited only for provenance of the revision track [1]. These examples should be read as protocol examples, not as empirical validation. Each one has the same structure: prepare candidate amounts, compute a declared gate, multiply before normalisation, and compare against a control or held-out reveal.

4.1 Three-History Survival Normalisation

The elementary probability example uses three equally prepared histories with accumulated losses

$$A_1 = 0, \qquad A_2 = 1, \qquad A_3 = 2. \tag{9}$$

The gate transmissions are

$$G_1 = 1, \qquad G_2 = e^{-1}, \qquad G_3 = e^{-2}. \tag{10}$$

After normalisation,

$$\mathbf{p} = \frac{(1, e^{-1}, e^{-2})}{1 + e^{-1} + e^{-2}} \approx (0.665,\ 0.245,\ 0.090). \tag{11}$$

This is the smallest example showing that probability enters after survival filtering. It is formal probability by normalisation, not primitive randomness.

4.2 Laser-Layer Component Exposure

The laser-layer example treats a weak selective layer with calibrated loss $\eta = 0.20$. Five prepared field states have exposed-support fractions

$$\mathbf{W} = (1.00,\ 0.75,\ 0.50,\ 0.25,\ 0.00). \tag{12}$$

The exposure-gated output is

$$G_{\mathrm{laser}}(W) = \exp(-0.20W), \tag{13}$$

giving

$$\mathbf{G}_{\mathrm{laser}} \approx (0.819,\ 0.861,\ 0.905,\ 0.951,\ 1.000). \tag{14}$$

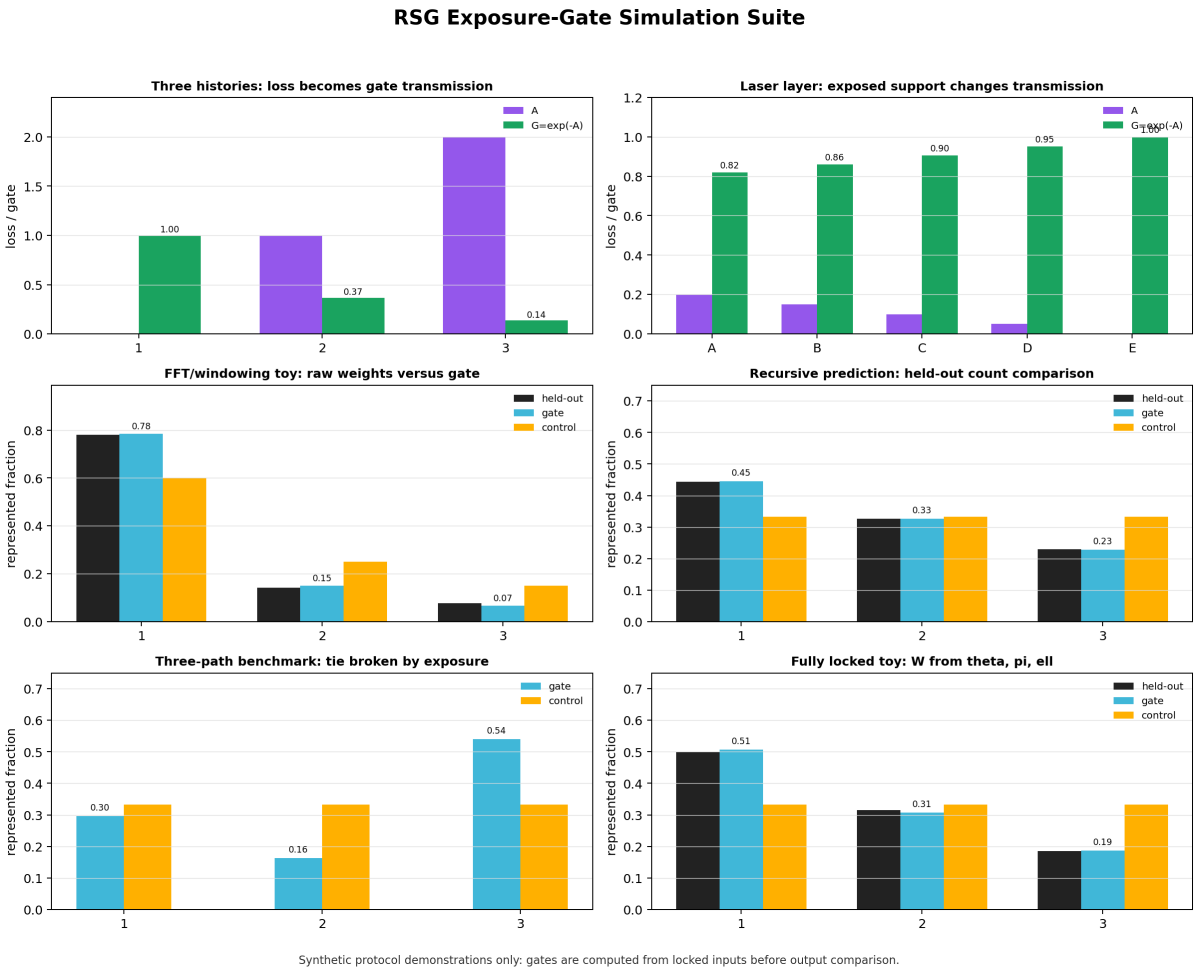

Figure 3: Overview of the numerical exposure-gate simulation suite. Each panel shows the same operational pattern: locked inputs determine a gate, and only the gated represented amounts are compared with a control or held-out readout.

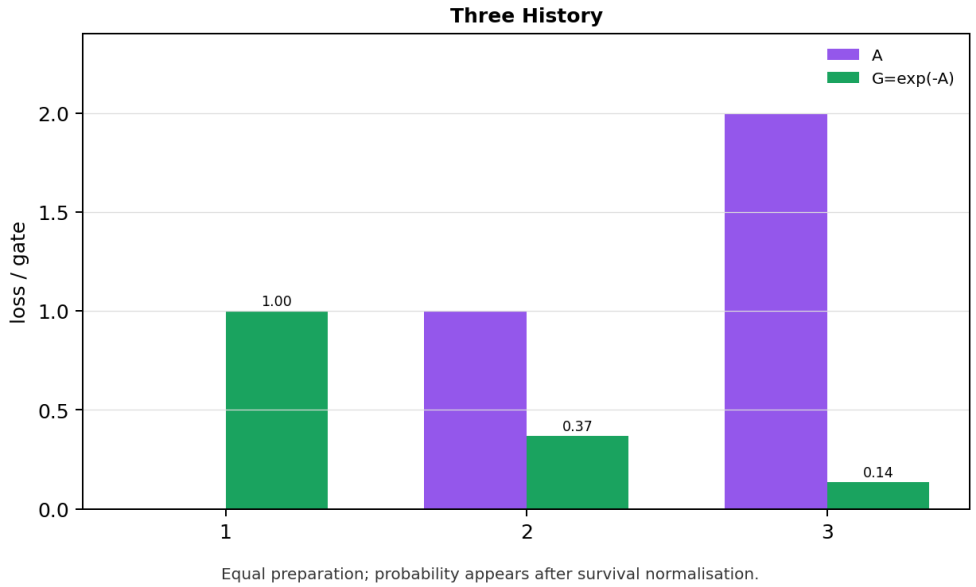

Figure 4: Three-history survival normalisation. The accumulated loss A_i determines the gate $G_i = \exp(-A_i)$, and the represented fractions are formed only after normalisation.

Ordinary path attenuation predicts the same transmission for every state,

$$G_{\text{path}} = \exp(-0.20) \approx 0.819. \tag{15}$$

With equal preparation, the represented exposure-gated fractions are

$$\mathbf{p}_{\text{laser}}^{\text{gate}} \approx (0.181,\ 0.190,\ 0.199,\ 0.210,\ 0.221), \tag{16}$$

whereas the path-only control gives the equal vector $(0.200, 0.200, 0.200, 0.200, 0.200)$. The example is useful because W has a direct support interpretation: only the component exposed to the selective layer is counted in the loss channel.

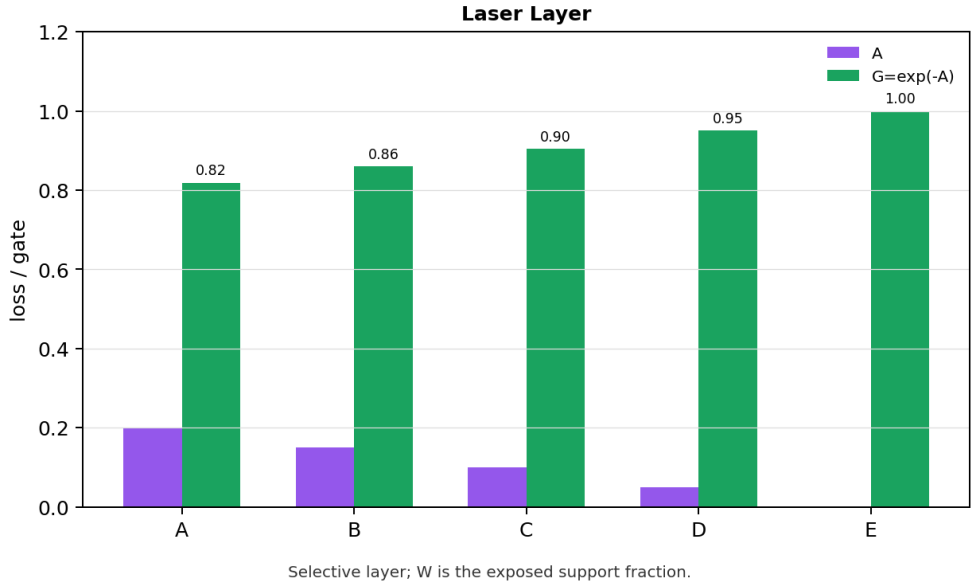

Figure 5: Laser-layer component exposure. A selective loss layer produces different gate transmissions because each prepared field state has a different exposed-support fraction W.

4.3 FFT Windowing Toy

The FFT/windowing toy uses raw preparation weights

$$\mathbf{q} = (0.60,\ 0.25,\ 0.15), \tag{17}$$

predeclared exposure values

$$\mathbf{W} = (0.05,\ 0.70,\ 0.95), \tag{18}$$

and common loss coefficient $\Gamma = 1.20$. The accumulated losses are

$$\mathbf{A} = \Gamma\mathbf{W} = (0.060,\ 0.840,\ 1.140). \tag{19}$$

The gate transmissions are

$$\mathbf{G} = e^{-\mathbf{A}} \approx (0.942,\ 0.432,\ 0.320), \tag{20}$$

and the gated surviving masses are

$$\mathbf{q} \odot \mathbf{G} \approx (0.565,\ 0.108,\ 0.048). \tag{21}$$

After normalisation,

$$\mathbf{p}^{\text{gate}} \approx (0.784,\ 0.150,\ 0.067). \tag{22}$$

For the held-out repeated-window reveal

$$\widehat{\mathbf{p}} = (0.781,\ 0.142,\ 0.077), \tag{23}$$

the total absolute error drops from

$$\sum_m |\widehat{p}_m - q_m| = 0.362 \tag{24}$$

to

$$\sum_m |\widehat{p}_m - p_m^{\text{gate}}| = 0.021. \tag{25}$$

The RMSE drops from 0.129 to 0.0076. The summed absolute log-ratio residual drops from 1.861 to 0.388. The correct claim is not that the gate replaces the FFT. The correct claim is that a locked survival-ranking layer can be compared with the raw preparation vector and, in this declared toy, matches the held-out output more closely.

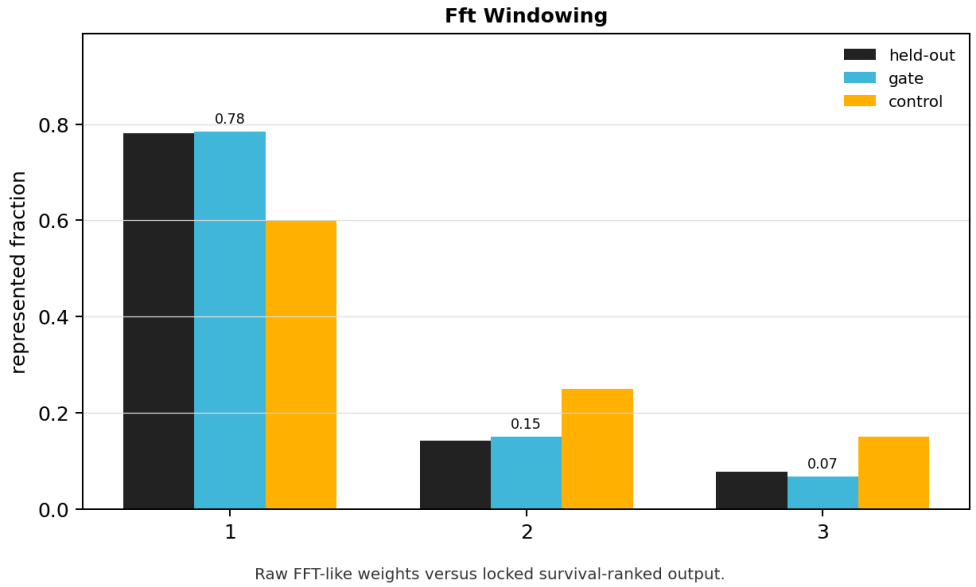

Figure 6: FFT/windowing toy. The raw preparation vector supplies the control, while the exposure-gated vector is judged against a held-out repeated-window reveal.

4.4 Recursive Prediction Toy

The recursive prediction toy uses three equal-preparation candidates with locked step multipliers

$$\mathbf{r}_1 = (0.90,\ 0.85,\ 0.80), \qquad \mathbf{r}_2 = (0.70,\ 0.82,\ 0.78), \qquad \mathbf{r}_3 = (0.95,\ 0.60,\ 0.55). \tag{26}$$

The survival weights are

$$\mathbf{S} \approx (0.612,\ 0.448,\ 0.314), \tag{27}$$

and the normalised prediction is

$$\mathbf{p}^{\text{gate}} \approx (0.446,\ 0.326,\ 0.228). \tag{28}$$

Against the held-out generated count fraction

$$\widehat{\mathbf{p}} = (0.444,\ 0.326,\ 0.230), \tag{29}$$

the uniform baseline has total absolute error 0.221, while the locked survival prediction has total absolute error 0.003.

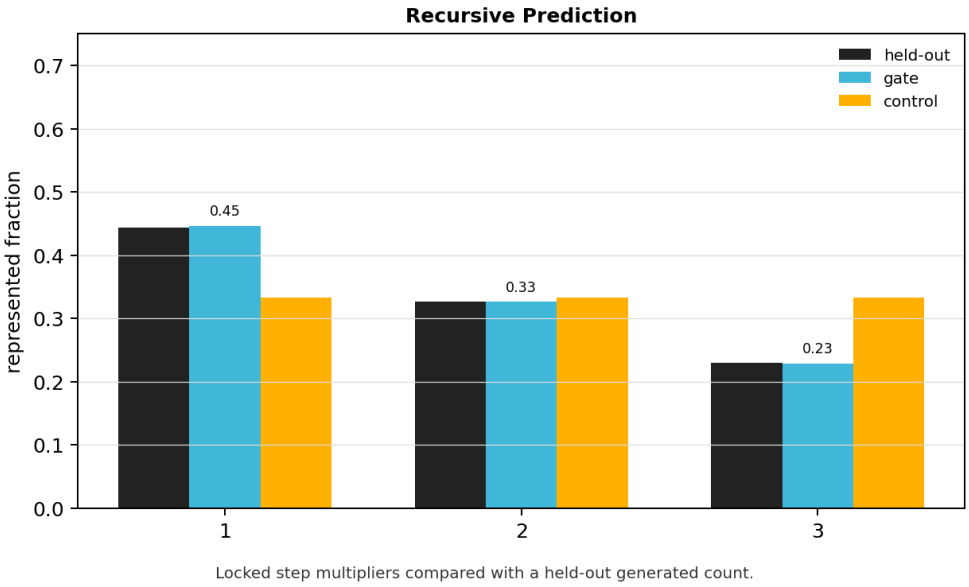

Figure 7: Recursive prediction toy. Locked step multipliers generate survival weights before the normalised prediction is compared with the held-out count fraction.

4.5 Three-Path Positive-Control Benchmark

The three-path benchmark fixes equal preparation, a common loss coefficient $\Gamma = 0.20$, a ten-layer duration, and mean exposures

$$(\bar{W}_1, \bar{W}_2, \bar{W}_3) = (0.50,\ 0.80,\ 0.20). \tag{30}$$

The accumulated losses are

$$\mathbf{A} = (1.00,\ 1.60,\ 0.40), \tag{31}$$

so the predicted vector is

$$\mathbf{p}_{\text{pred}} \approx (0.297,\ 0.163,\ 0.541). \tag{32}$$

The ordinary attenuation control gives a tie if the ordinary path loss is the same for all paths. The gate model instead predicts the ordering $p_3 > p_1 > p_2$, because the exposed loss differs between paths.

4.6 Fully Locked Toy Protocol

The fully locked toy protocol uses three equal-preparation channels, ten layers, $\Delta t = 1$, $I_{i,0} = 1$, and $\Gamma = 0.20$. It sets $\ell = 1$, $\Pi_{i,k} = 1$, and

$$\Theta_{1,k} = \sqrt{\frac{1}{3}}, \qquad \Theta_{2,k} = 1, \qquad \Theta_{3,k} = \sqrt{3}. \tag{33}$$

Using

$$W_{i,k} = \frac{\Theta_{i,k}^2}{\Theta_{i,k}^2 + \ell^2 \Pi_{i,k}^2}, \tag{34}$$

the locked exposures are

$$\mathbf{W} = (0.25,\ 0.50,\ 0.75). \tag{35}$$

The accumulated losses after ten layers are

$$\mathbf{A} = (0.50,\ 1.00,\ 1.50), \tag{36}$$

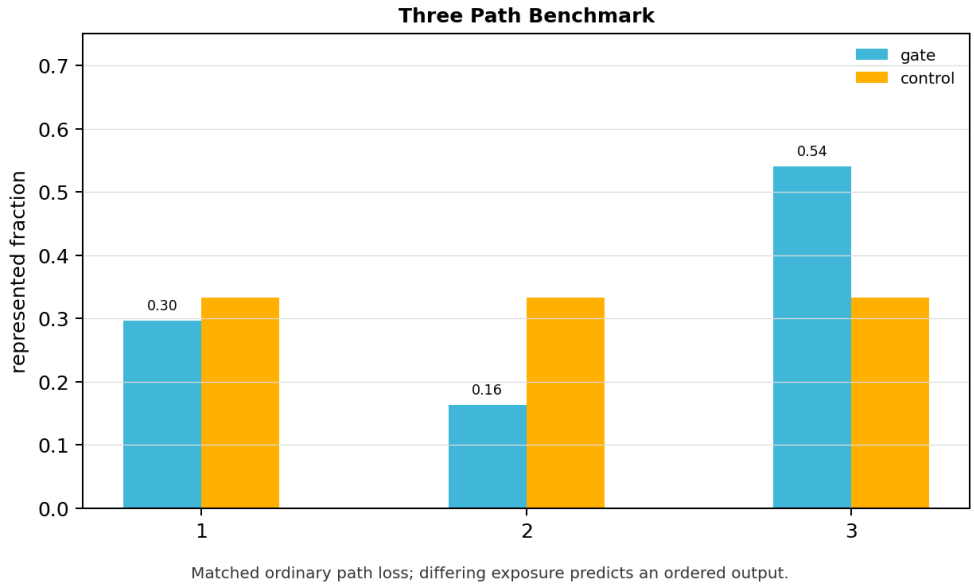

Figure 8: Three-path positive-control benchmark. Ordinary attenuation predicts a tie, while the exposure-gated model breaks the tie because the locked exposures differ.

and the locked gate prediction is

$$\mathbf{p}_{\text{pred}} \approx (0.506,\ 0.307,\ 0.186). \tag{37}$$

The ordinary attenuation control predicts $(1/3, 1/3, 1/3)$. The example demonstrates operational distinguishability and non-ad hoc computation of W, not laboratory validation.

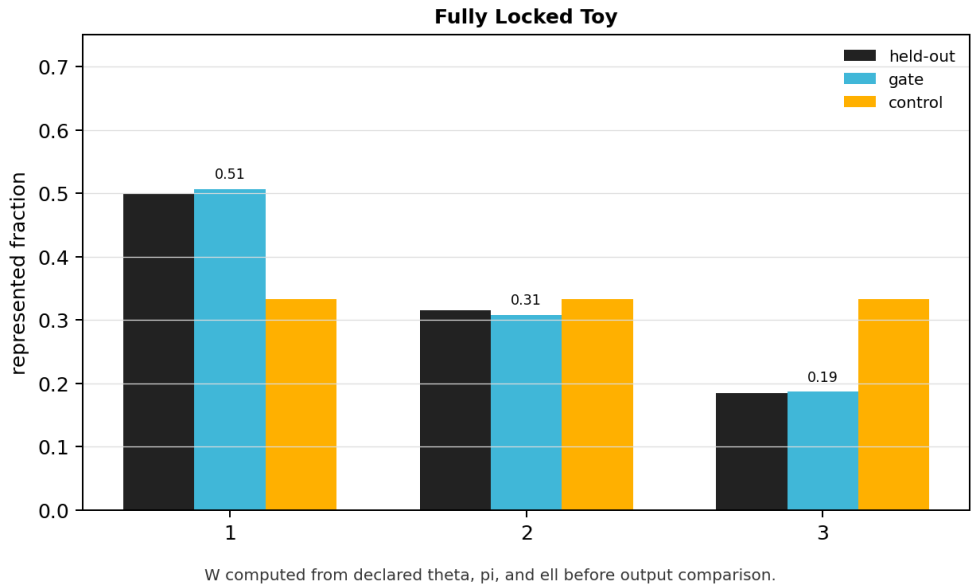

Figure 9: Fully locked toy protocol. The exposure W is computed from the declared Θ, Π, ℓ convention before the output vector is compared with the ordinary attenuation control.

Demonstration	Fixed input	Output readout
Three-history normalisation	$A = (0, 1, 2)$, equal preparation	$p \approx (0.665, 0.245, 0.090)$.
Laser-layer check	$W = (1, 0.75, 0.50, 0.25, 0)$, $\eta = 0.20$	$G \approx (0.819, 0.861, 0.905, 0.951, 1.000)$.
FFT/windowing toy	$q = (0.60, 0.25, 0.15)$, $W = (0.05, 0.70, 0.95)$, $\Gamma = 1.20$	Total absolute error improves from 0.362 to 0.021.
Recursive prediction toy	Step multipliers fixed before reveal	Total absolute error improves from 0.221 to 0.003.
Three-path benchmark	Common $\Gamma = 0.20$, differing exposure	Predicts $p_3 > p_1 > p_2$ rather than a tie.
Fully locked toy protocol	$W = (0.25, 0.50, 0.75)$ computed from Θ, Π, ℓ	Predicts $(0.506, 0.307, 0.186)$, not $(1/3, 1/3, 1/3)$.
Beam-mask demo	W computed by pixel summing incident support in fixed masks	Total absolute error improves from 2.428 to 0.030.
Surtea support demo	$W_X = \nu_D(\mathrm{bd}_D X)/\nu_D(\mathrm{cl}_D X)$	Boundary-heavy supports receive lower gate transmission.

5 Relation to the Probability Layer

The gate notation used here is the same operational count map used in the probability note and the v1.4 RSG manuscript. A prepared represented amount is

$$C_{i,0} = C_0 q_i. \tag{38}$$

After exposure-gate transmission,

$$C_{i,N} = C_0 q_i G_i. \tag{39}$$

The represented output fraction is then

$$p_i = \frac{C_{i,N}}{\sum_j C_{j,N}} = \frac{q_i G_i}{\sum_j q_j G_j}. \tag{40}$$

The gate is therefore not a second probability law. It is the multiplier that acts before normalisation. The term probability enters only after the transmitted represented amounts are divided by their total.

6 Reproducibility

The executable notebook associated with this companion note is:

`https://colab.research.google.com/drive/1OdMRGMMT6uDoDETVRt0awemPj-ZoSIZW?usp=sharing`.

The notebook is cited as the reproducibility reference for the rendered beam-mask and Surtea support demonstrations [4]. The Colab code is deliberately trig-free: it does not use sine, cosine, tangent, or inverse-trigonometric functions. The numerical cases drawn from the probability note and the v1.2 revision are recorded above as fixed examples. They are intended to demonstrate the locked calculation pattern, not to replace a laboratory measurement.

References

[1] P. M. Austin, *Recursive Survival Geometry v1.2*, rejected manuscript, Information Physics Institute, 2026.

[2] P. M. Austin, *Surtea-Austin Triangle*, internal manuscript, Information Physics Institute, 2026.

[3] P. M. Austin, *Probability in Recursive Survival Geometry: Survival Normalisation, Representation Measure, and Analogue Readout*, Information Physics Institute, 2026.

[4] P. M. Austin, *Exposure-Gate Beam-Mask Demonstration: Colab Notebook*, Information Physics Institute, 2026. Available at: `https://colab.research.google.com/drive/1OdMRGMMT6uDoDETVRtOawemPj-ZoSIZW?usp=sharing`.

[5] National Instruments, *Understanding FFTs and Windowing*, technical note. Available at: `https://download.ni.com/evaluation/pxi/Understanding%20FFTs%20and%20Windowing.pdf`.

[6] A. N. Kolmogorov, *Foundations of the Theory of Probability*, Chelsea Publishing Company, 1956.

[7] C. E. Shannon, "A mathematical theory of communication," *Bell System Technical Journal*, vol. 27, pp. 379–423 and 623–656, 1948.